energies

MDPI

Article

Reservoir Characteristics and Shale Oil Enrichment of Shale Laminae in the Chang 7 Member, Ordos Basin

Mengying Li [1], Wenzheng Li [1], Mingfeng Gu [1], Songtao Wu [2], Pengwan Wang [1], Yuce Wang [1], Quanbin Cao [1], Zhehang Xu [1] and Yi Hao [1,*]

[1] PetroChina Hangzhou Institute of Petroleum Geology, Hangzhou 310023, China; limy_hz@petrochina.com.cn (M.L.)
[2] Research Institute of Petroleum Exploration and Development (RIPED), China National Petroleum Corporation (CNPC), Beijing 100083, China; wust@petrochina.com.cn
* Correspondence: limy0301@163.com

Abstract

The laminae of lacustrine shale in China have been systematically identified and characterized by a combination of core/slice observations, mineral compositions, geochemical analysis, pore structure characterization, and oil-bearing evaluation. The shale of the Chang 7 Member, Yanchang Formation, Ordos Basin was examined as an example in the study. Four types of laminae are developed in the Chang 7 Member, including felsic laminae (FQL), clay laminae (CLL), organic matter laminae (OML), and tuff laminae (TUL). The shale reservoirs exhibit significant heterogeneity. Of these, FQL and TUL have superior reservoir characteristics. The pore diameter of TUL is primarily composed of micrometer-sized secondary pores that are generated during the diagenesis process, while mesopore and macropore development are dominant in FQL. The main source laminae in the Chang 7 Member of the Ordos Basin are the OML and CLL, while the main reservoir laminae are the FQL and TUL. Some of the hydrocarbons produced by hydrocarbon generation are stored in the pore space inside the laminae, while the majority migrate to the inorganic pores of the adjacent FQL and TUL. It confirms that OML and CLL afford abundant shale oil, the combination of organic pores and inorganic pores in FQL and TUL serve as reservoir space, and the "clay generation-siliceous reservoir" shale oil enrichment model is established in the Chang 7 Member of Ordos Basin.

Keywords: laminae structure; enrichment model; fine-grained sediment; shale oil; Chang 7 Member; Ordos Basin

check for updates

Academic Editor: S.M. Farouq Ali

Received: 27 July 2025
Revised: 12 September 2025
Accepted: 27 September 2025
Published: 10 October 2025

Citation: Li, M.; Li, W.; Gu, M.; Wu, S.; Wang, P.; Wang, Y.; Cao, Q.; Xu, Z.; Hao, Y. Reservoir Characteristics and Shale Oil Enrichment of Shale Laminae in the Chang 7 Member, Ordos Basin. *Energies* **2025**, *18*, 5342. https://doi.org/10.3390/en18205342

Copyright: © 2025 by the authors. Licensee MDPI, Basel, Switzerland. This article is an open access article distributed under the terms and conditions of the Creative Commons Attribution (CC BY) license (https://creativecommons.org/licenses/by/4.0/).

1. Introduction

Low porosity, ultra-low permeability, and poor mobility are characteristics of continental shale reservoirs. The availability of reservoirs, including their physical attributes, oil bearing capacity, and movability, is crucial for shale oil exploration and development. It also plays a major role in determining the development of the shale oil "sweet spot" [1,2]. The laminae are the most distinctive sedimentary structure of the shale series, which have been proved to be widely developed in shale [3]. The discovery of the 1-billion-ton Qingcheng shale oil field in 2019 realized a new breakthrough in the risky exploration of shale oil of the Yanchang Formation in the Ordos Basin. In 2021, the proven reserves of shale oil in the Yanchang Formation reached 11.52×10^8 t, and the annual production of shale oil amounted to 188×10^4 t, which demonstrated the scale-effective development of shale oil in the Ordos Basin.

The primary shale series in the Yanchang Formation is called the Chang 7 Member. Currently, millimeter-scale laminae research is lacking in the study of reservoir effectiveness in the Chang 7 Member, which is mostly reliant on lithofacies as the most fundamental research object, primarily on the centimeter-decimeter scale. The development of laminae is the result of the joint action of early sedimentation and late diagenesis [4–10]. The emergence of shale laminae directly affects the availability of shale oil reservoirs [11,12]. The type, thickness, pore structure, and combination of laminae are the main factors that determine the quality of source rock and reservoir, and the shale oil micromigration. Current research indicates that, while researchers abroad focus on the morphology, continuity, and geometric relationship of laminae, the mineral composition, lamina combinations, and laminae porosity of shale series in an independent sedimentary environment are the counterparts in China [13–19]. There is currently an absence of knowledge of the characteristics of shale laminae and the relationship between the lamina and shale oil enrichment. Therefore, it is of great significance to carry out a detailed study of the laminae structure, elucidate the types and pore characteristics of laminae, and explore the micromigration mechanism of shale oil under the control of laminae, so as to establish an oil enrichment model for fine-grained sedimentary shale oil in the Chang 7 Member of Ordos Basin. It is vital for supporting the exploration and development of shale oil.

2. Geological Setting

With a sedimentary area of approximately 25×10^4 km^2, the Ordos Basin is the second biggest Mesozoic basin in China (Figure 1). With a stratigraphic thickness of roughly 1300 m, the continental river-delta-lacustrine facies sedimentary system originated from the Triassic Yanchang Formation. The basin experienced a rapid period of geological subsidence during the depositional period of the Chang 7 Member of Yanchang Formation. This subsidence displayed north–south disequilibrium and asymmetry, and it ultimately resulted in the base of the basin displaying the spreading pattern of "steep in the south and ease in the north". The largest expansion period occurred during this time, when the lake grew to be large and deep. A set of dark mudstone and black shale series of a semi-deep and deep lacustrine face, with a thickness of up to 100 m, is widely overlaying and developed during this time, laying the foundation for the Mesozoic continental oil production.

Research into Chinese shale oil is currently focused on the organic matter-rich shale series in the Chang 7 Member in the Ordos Basin. The organic matter is primarily II1 type, Ro values range from 0.6% to 1.0%, and S_1 is 1 to 10 mg/g in the Chang 7 Member. The organic matter content ranges from 0.8% to 22%, with the highest concentration in the center of the basin. The amount of organic matter decreases vertically as it moves up and down, and the organic carbon content of Chang 7_3 Member is significantly higher than that of Chang 7_1 Member and Chang 7_2 Member. The shale in Chang 7 Member has an oil content ranging from 2% to 7%, indicating that its quality has reached medium preference and that there is a broad prospect for further exploration and development.

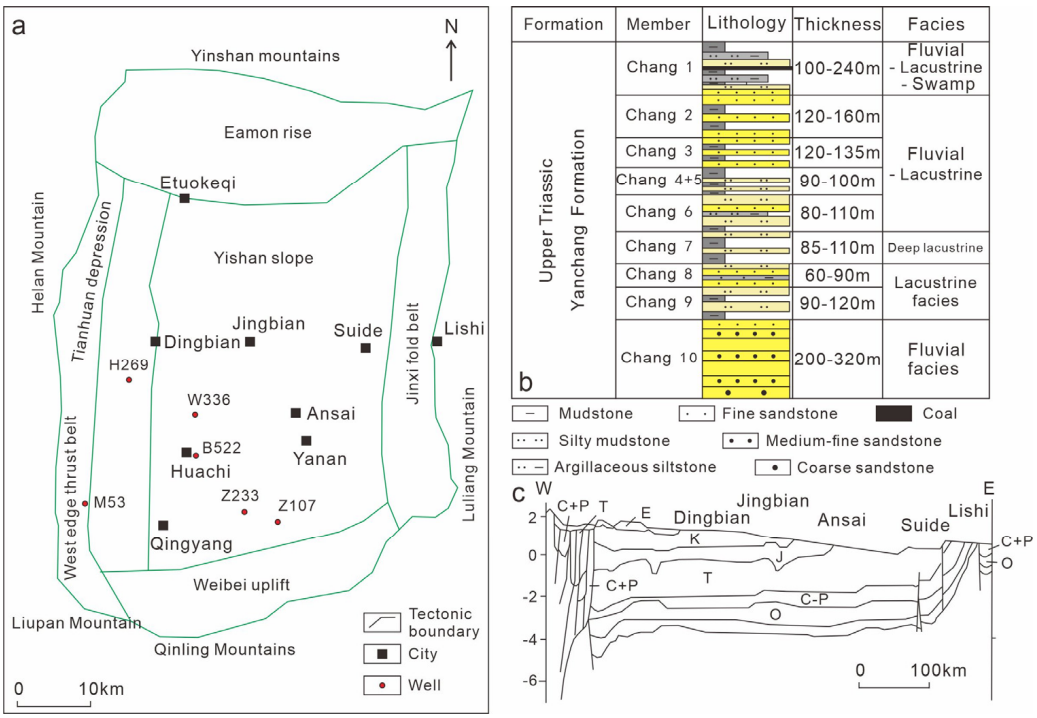


Figure 1. Tectonic division, stratum, and east–west profile in Ordos Basin. (**a**) Tectonic division in Ordos Basin; (**b**) Stratum in Ordos Basin; (**c**) The east–west profile in Ordos Basin.

3. Materials and Methods

To analyze the characteristics of laminae in the Chang 7 Member, 55 core samples of centimeter-decimeter scale were collected. All the samples were analyzed using X-ray fluorescence spectrometry and slice observation to obtain the element compositions and laminae characteristics of the whole cores. Wire-electrode cutting was used to cut the samples for fine study into laminae. These were analyzed for geochemical characteristics, mineralogical composition, and pore structures using TOC content measurement, rock pyrolysis analysis, X-ray diffraction analysis, Qemscan, nitrogen adsorption, NMR porosity measurement, Modular Automated Processing System, FIB-SEM, and nano-CT technology.

The laminae and their combinations were identified using core description, slice observation, X-ray fluorescence spectrometry, and mineral compositions. Element compositions were determined using a table-X-ray fluorescence spectrometry (XRF) at the National Energy Tight Oil and Gas Research and Development Center. A BrukerM4 TORNADO high-performance micro-area X-ray fluorescence spectrometer (detection limit 5×10^{-6}) from Bremen, Germany was used to obtain the qualitative and quantitative characteristics of various elements, which were scanned in 20 μm increments. Elements such as K, Na, Ca, Mg, Al, Si, Fe, and S were extracted for fine identification and characterization of the types and combinations of laminae.

4. Results

4.1. Types and Combinations of Laminae

Four types of laminae are developed in the Chang 7 Member, including felsic laminae (FQL), clay laminae (CLL), organic matter laminae (OML), and tuff laminae (TUL), according to analyses of 81 core samples of laminae scale from wells Huang 269, Wu 336, Zhuang 233, and Zheng 107 using XRF scanning and LSCM scanning in conjunction with polarized light microscope observation and XRD mineral composition testing (Figure 2). Its low carbonate mineral composition is insufficient for the development of carbonate laminae. Studies showed that, in contrast to the FQL and CLL, the potassium feldspar

content in the TUL is higher than the plagioclase content. Furthermore, concerning the primary minerals, feldspathic minerals with contents typically exceeding 50% predominate in the FQL, whereas the clay minerals in the CLL have higher contents than other laminae (generally exceeding 40%), which are primarily composed of andreattite and illite; the pyrite content is primarily 15% to 35% in the OML, which is significantly higher than that of the other laminae (the pyrite content of <10%).

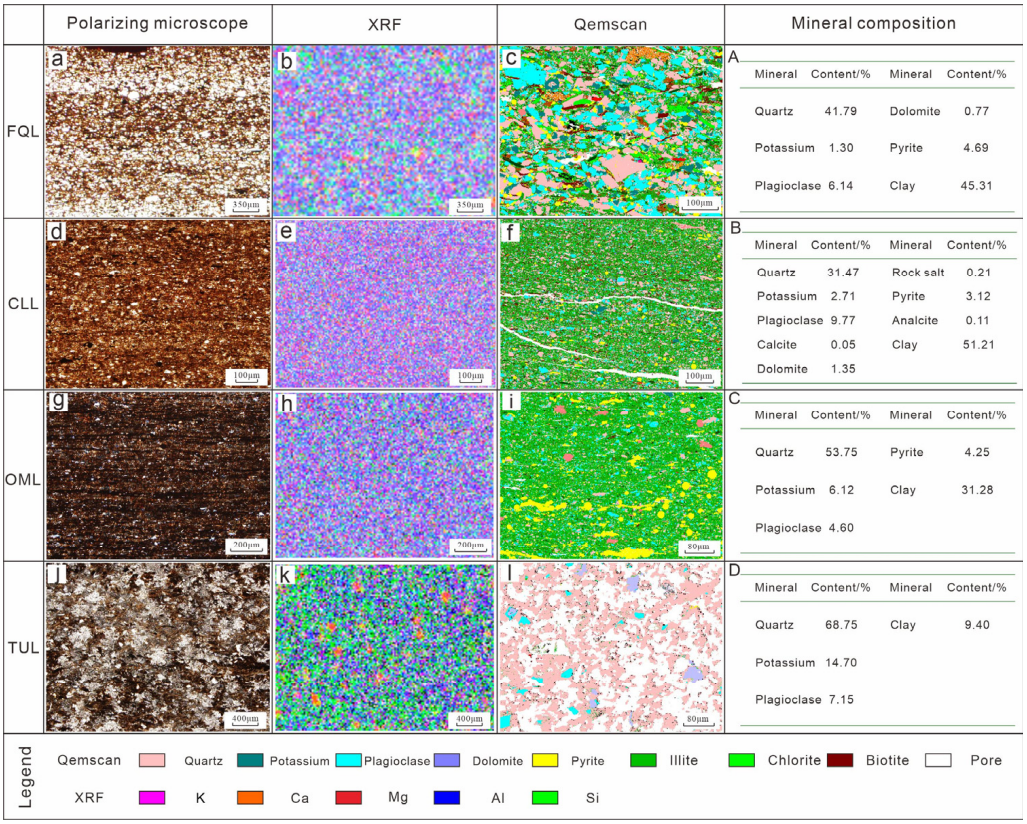


Figure 2. Lamina types and characteristics of the Chang 7 Member in Ordos Basin. (**a**–**c**) FQL, Well W336, 1969.7 m; (**d**–**f**) CLL, Well W336, 2060.5 m; (**g**–**i**) OML, Well Z233, 1789.5 m; (**j**–**l**) TUL, Well W336, 1960.1 m. (**A**–**D**) The mineral composition data are derived from the measured results of the corresponding samples.

(1) Felsic laminae: It is colorless under single polarized light, and exhibits a mixed size particle (Figure 2a), with a thickness ranging from hundreds of microns to centimeters. The FQL are dominated by sodium feldspar, potassium feldspar, quartz, and clay minerals. The clay minerals are primarily immonite, illite, and chlorite, which are dispersed along the laminae (Figure 2b,c). The biotite is substantially developed and dispersed, and the isolated distributions of monocrystalline pyrite are observed with the majority of pyrite particle sizes ranging between 2 and 10 μm.

(2) Clay laminae: The CLL is the predominant type of the Chang7 shale, which has a brownish-brown color in single-polarized light, a high proportion of grain frequency, and thickness ranging from a few tens of micrometers to centimeters (Figure 2d). The CLL are dominated by clay minerals, quartz, and feldspar (Figure 2e,f). The clay minerals are primarily immonite, illite, and chlorite, which are dispersed along the laminae. CLL are in gradual or abrupt contact when interbedded with FQL and when interbedded with OML and DOL, they showed abrupt contact.

(3) Organic matter laminae: It is dark or black in single-polarized light, with good continuity and a large thickness (Figure 2g). The mineral composition is dominated by clay minerals, pyrite, and quartz, and the clay minerals are mainly andreattite and illite (Figure 2h). A large number of organic matter bands are visible within the OML, with the main organic matter bands ranging from 3 to 10 μm in thickness and developing continuously and in bedding distribution. Pyrite is densely distributed within the OML, including monolithic pyrite, lenticular pyrite aggregate, and pyrite framboids (Figure 2i). Apatite is seen to be developed in the OML, which is predominantly globular in shape and partially filled by organic matter.

(4) Tuff laminae: The TUL, serving as a typical lamina in the Chang 7 Member of the Ordos Basin, is well developed in shale series of the freshwater condition. It is grayish-white in single polarized light (Figure 2j), and the thickness varies from a few hundred micrometers to centimeters. The morphological feature is relatively flat and straight, and it shows gradual or abrupt contact when it is interlayered with the OML. The TUL are dominated by quartz, feldspar, clay minerals, and siderite, and some samples contain only a small amount of clay minerals and siderite (Figure 2k,l).

The Chang 7 shale developed four distinct types of laminae combinations: the FQL–CLL combination, the FQL–OML combination, the CLL–OML combination, and the TUL–OML combination (Figure 3). Mineral particle sizes recorded in the FQL–CLL combination show an asymptotic decrease in particle size, with smaller values at the CLL's farther-from-the-FQL locations. (Figure 4).

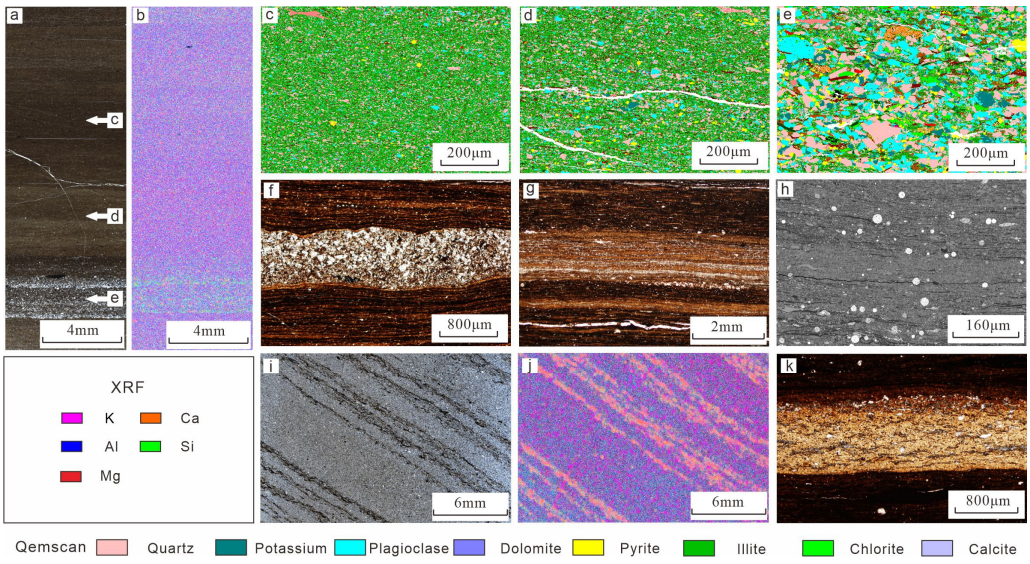


Figure 3. Lamina combinations of the Chang 7 Member in Ordos Basin. (**a**) FQL–CLL combination, polarizing microscope, Well W336, 1969.7 m; (**b**) FQL–CLL combination, XRF, Well W336, 1969.7 m; (**c**) CLL, polarizing microscope, Well W336, 1969.7 m; (**d**) CLL, polarizing microscope, Well W336, 1969.7 m; (**e**) FQL, polarizing microscope, Well W336, 1969.7 m; (**f**) FQL–OML combination, polarizing microscope, Well Z233, 1789.5 m; (**g**) CLL–OML combination, polarizing microscope, Well Z107, 1134.2 m; (**h**) OML, SEM observation, Well Z107, 1134.2 m; (**i**) TUL, polarizing microscope, Well W336, 1960.1 m; (**j**) TUL, XRF, Well W336, 1960.1 m; (**k**) TUL–OML combination, polarizing microscope, Well W336, 2021.4 m.

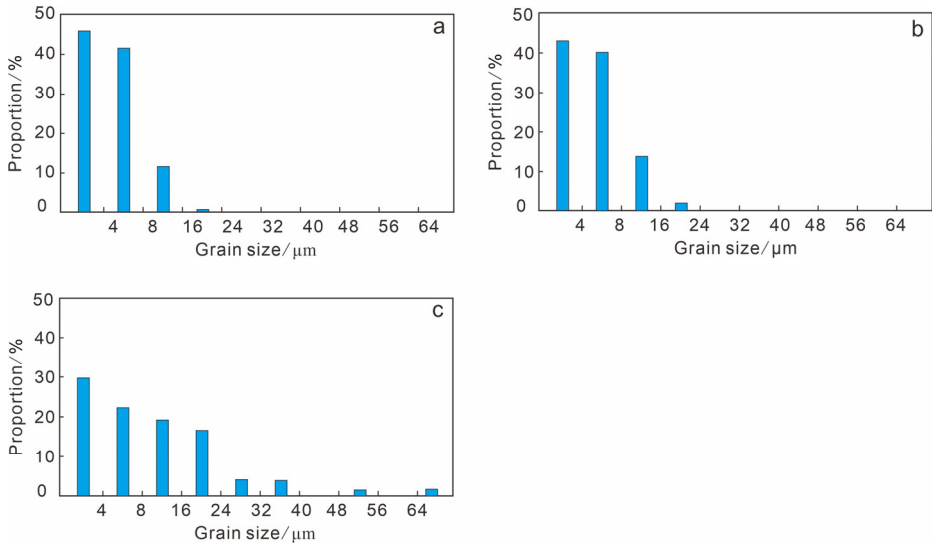


Figure 4. Grain size of FQL–CLL combination ((**a**–**c**) correspond to Figure 2c–e respectively).

4.2. Pore Characterization of Shale Laminae

The shale series of the Chang 7 Member in the Ordos Basin are dominated by dissolution pores, intragranular pores, organic pores, and microfractures (Figure 5). The dissolution pores primarily consist of feldspar and organic pores, the intragranular pores predominantly include pyrite and clay mineral pores, and the microfractures are generally comprised of organic matter shrinkage fractures and structural microfractures.

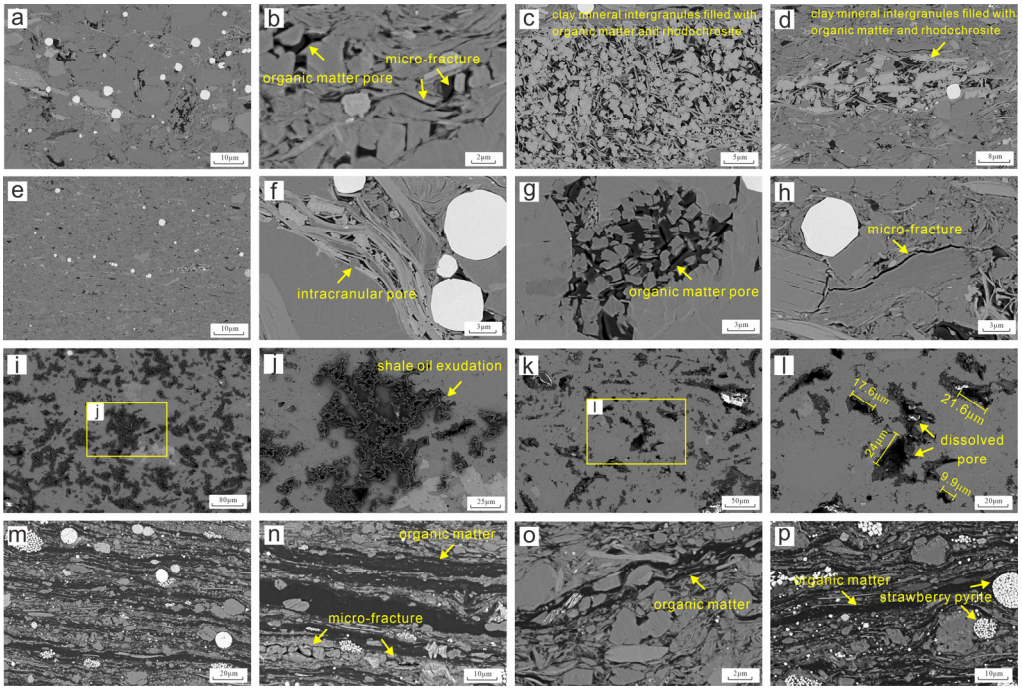


Figure 5. Pore structure of the Chang 7 Member in Ordos Basin. (**a**–**d**) FQL, Well W336, 1969.7 m; (**e**–**h**) CLL, Well W336,1969.7 m; (**i**–**l**) TUL, Well W336,1960.1 m; (**m**–**p**) OML, Well H269, 2511.0 m.

The predominant pore types found in the FQL are microfractures, feldspar dissolution pores, and clay mineral intragranular pores (Figure 5a–d). However, the dissolution pores are primarily filled with kaolinite and organic matter, while the clay mineral intragranular pores are filled with organic matter and cemented with rhodochrosite. The microfractures are mainly the edge fractures of mica particles, feldspar, pyrite, and other minerals, which have

a high degree of development. The predominant pore types found in CLL are intragranular pores and microfractures, both of which are typically filled with siderite and organic matter. The majority of microfractures are structural fractures, with a tiny number of edge fractures in clay minerals (Figure 5e–h). The TUL experiences devitrification, forming a large number of secondary dissolved pores that serve as a suitable reservoir. Under SEM, a significant amount of shale oil leaked out and was adsorbed near the edge of the dissolved pores (Figure 5i–l). The organic pores and microfractures, as well as the infrequent dissolution and intergranular pores, are among the less developed intragranular pores of the OML (Figure 5m–p), but the OML has a significant concentration of apatite and pyrite.

4.2.1. Pore Morphology

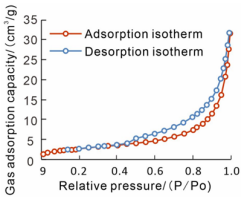
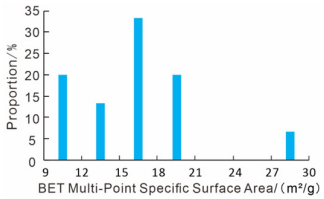
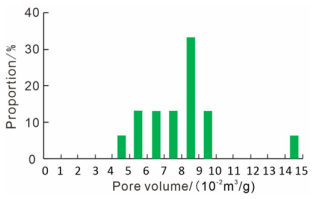
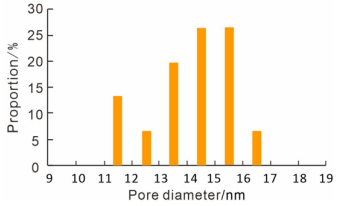
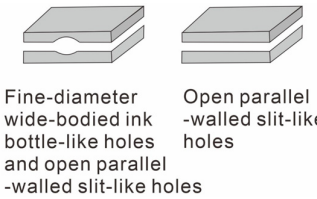
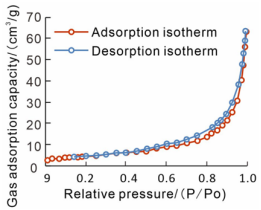
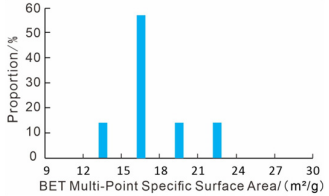
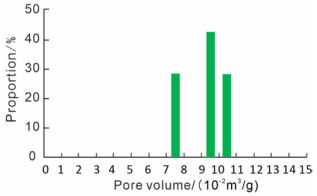
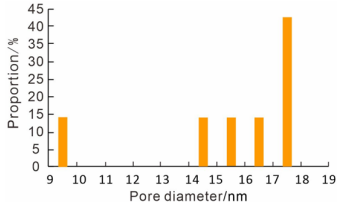
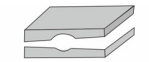
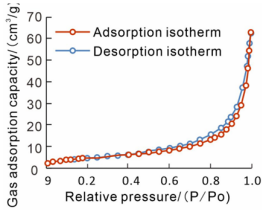
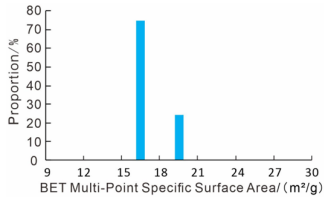
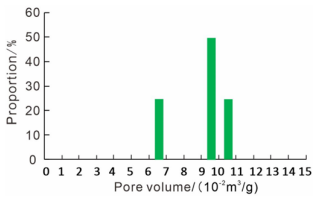
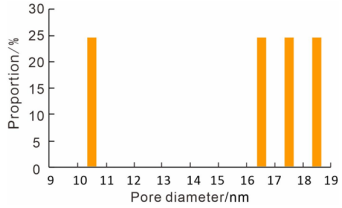
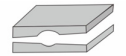
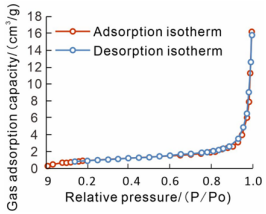
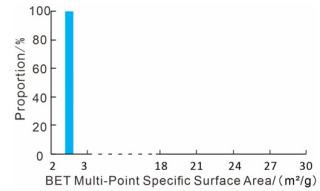
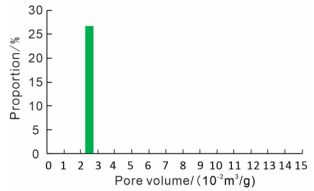
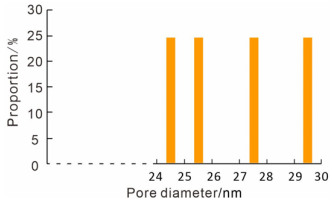
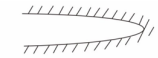
The study combined nitrogen adsorption and scanning electron microscopy to thoroughly measure the pore morphology of shale laminae in the Chang 7 Member of the Ordos Basin (Table 1). The mesopore (2~50 nm) morphology of the laminae in the shale series of the Chang 7 Member is categorized and characterized based on the nitrogen adsorption measurement (Table 1). As compared to the other laminae, the desorption curve had a stronger upward concavity in CLL. The hysteresis ring is larger and the results clearly demonstrate desorption and coagulation, indicating that the overall pore structure is mostly composed of parallel slit-like holes and fine-diameter, wide-bodied ink-bottle pores in CLL. This is the combined reservoir space of the mineral edge seams and clay mineral intragranular pores. The upward concavity in the FQL and OML desorption curves is also evident, but it is less pronounced than in CLL, with smaller hysteresis loops and no discernible decoagulation phenomena. It indicates that open wedge-shaped and curvilinear slit-like pores predominate in the FQL and OML. These pores reveal the storage space with a combination of intraparticle pores, dissolution pores, and microfractures of clay minerals. The tiny difference between the TUL desorption and adsorption curves indicates that there is no evaporation or decoagulation process and that closed slit-like holes predominate at one end of the TUL storage space. It is made up primarily of closed, slit-like pores.

4.2.2. Pore Size Distribution

The study conducted joint pore size characterization experiments using scanning electron microscopy (SEM), MAPS image acquisition and splicing (mesopore 2~50 nm; macropores >50 nm), nuclear magnetic resonance (macropores > 50 nm), and nitrogen adsorption (mesopore 2~50 nm) to comprehensively characterize the pore size distribution of laminae. The results of these experiments are used to characterize the pore size of CLL, FQL, and OML. The MAPS image acquisition and splicing approaches are used to characterize the pore size of CLL, FQL, and OML. Finally, the information is summarized and analyzed, taking into account that the TUL samples are not tested despite having clear free oil seepage characteristics.

The pores of FQL are mostly mesopores and macropores, according to NMR data, and the pore size distribution exhibits bimodal features. The peak, which contributes primarily to the combined FQL porosity, is located at 8 nm and 581 nm, respectively. The majority of the pores of CLL are mesopores and macropores, with a bimodal pore size distribution. The peak of the porosity is located at 13 nm and 581 nm, respectively, and the mesoporous range makes up the greatest portion of the porosity. The primary contributors to OML are mesopores and macropores. The pore size of OML exhibits triple-peak features, with peak pore sizes of 11 nm, 518 nm, and 10,982 nm, respectively. However, the mesopore range accounts for the majority of pore contributions. The pore size distribution of TUL displayed a three-peak pattern, with peak pore sizes of 8 nm, 452 nm, and 12,542 nm, respectively. Macropores predominated and are supplemented by mesopores.

Table 1. Pore structure of the Chang 7 Member in Ordos Basin.

Laminae	Main Type	Adsorption Desorption Curve	Pore Structure Characterization			
			BET Multi-Point Specific Surface Area	Pore Volume	Pore Diameter	Pore Morphology
CLL	I					
FQL	II					
OML	III					
TUL	IV					

The pore size distribution data for CLL, FQL, and OML in freshwater conditions demonstrate that all three types of laminae have more mesopores than 90%, which is much more than the other pore sizes (Figure 6). The pore size of 50~500 nm primarily contributes to the porosity of the CLL, the pore size of 100 nm or more primarily provides the porosity of the FQL, and the pore size of more than 1000 nm primarily leads to the porosity of the OML.

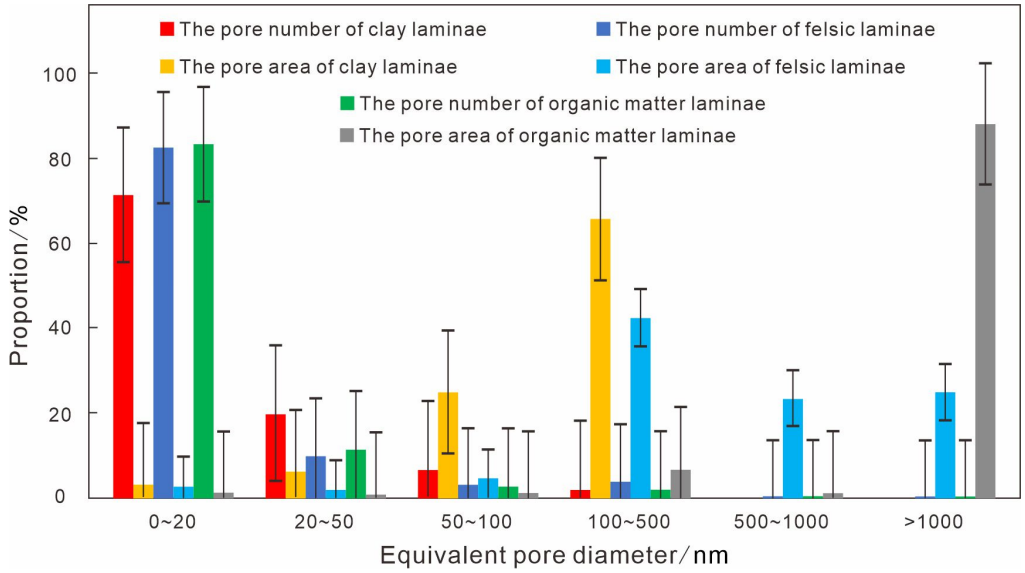


Figure 6. Pore size characteristics by MAPS of the Chang 7 Member in Ordos Basin.

The mesopore pore size distribution is further analyzed using nitrogen adsorption experiments, and the mesopore pore sizes exhibited TUL > OML > FQL > CLL (Table 1), with an average pore size distribution range of 24~30 nm, 16~19 nm, 14~18 nm, and 11~17 nm, respectively.

4.2.3. Porosity

The present study intends to provide a comprehensive characterization of the porosity of the lamiane of the shale series in the Chang 7 Member of the Ordos Basin. To this end, joint pore characterization experiments using nuclear magnetic resonance, MAPS splicing technique, and scanning electron microscopy have been conducted. The results have been analyzed and summarized.

The Chang 7 Member of the Ordos Basin has the following porosity in its shale series: TUL (averaging 14.84%) outperformed FQL (averaging 4.25%), CLL (averaging 2.35%), and OML (averaging 2.17%), with the TUL having clear benefits. Mesopores and macropores accounted for the majority of pores in shale laminae (Figure 7). Using the MAPS technique, the pore plane porosity is examined. The results showed that FQL > CLL > OML, with the pore plane porosity of CLL, FQL, and OML being 0.206%, 0.514%, and 0.004%, respectively. These results are consistent with the conclusion drawn from the NMR data.

After an extensive evaluation, it was determined that shale laminae of the Chang 7 Member in the Ordos Basin has porosity that is TUL > FQL > CLL > OML. TUL is characterized by a large pore radius and a preponderance of micrometer-sized pores (Figure 7), primarily composed of numerous secondary pores generated during the diagenesis process. Both macro- and meso-pore development in FQL is superior. Micro-nanometer-sized pores, primarily dissolution pores, clay mineral intragranular pores, organic matter pores, and microfractures, predominate in macro- and meso-pore development. Macroscopic and mesopores predominate in CLL and OML, with mesopores contributing more to porosity

than macropores in FQL. Micro- and nanoscale pores are mostly made up of clay mineral intragranular pores, organic matter pores, and microfractures. Fractures may be the cause of the macropores contribution in OML. Mesopores predominate in every lamina in terms of quantity, and the overall presentation demonstrates that while macropores, which do not dominate in number, contribute more porosity, mesopores only contribute a small percentage of the porosity.

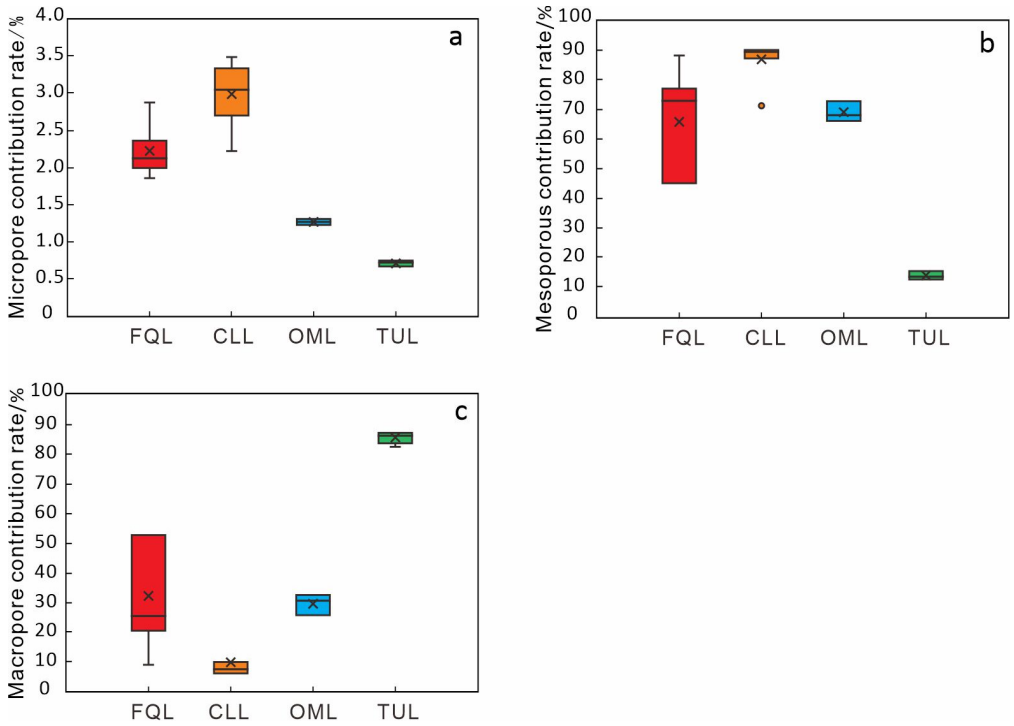


Figure 7. Contribution of different pore sizes to porosity of shale laminae of the Chang 7 Member in Ordos Basin. (**a**). Contribution of micropores to porosity in laminae of the Chang 7 Member of the Ordos Basin; (**b**). Contribution of mesopores to porosity in laminae of the Chang 7 Member of the Ordos Basin; (**c**). Contribution of macropores to porosity in laminae of the Chang 7 Member of the Ordos Basin.

4.3. Micromigration Mechanisms and Enrichment Model of Shale Oil

The laminae of the shale series in the Chang 7 Member of the Ordos Basin have been evaluated using NMR oil-bearing test data. The results indicate that the laminae have an oil saturation of TUL (74.72%) > OML (52.47%) > FQL (44.17%) > CLL (39.2%) (Figure 8). The TUL and OML signals are significantly stronger than those of the other laminae. The movable oil saturation of TUL is 63.45%, and the oil-bearing volume (relative) is highest at 0.5359%. The movable oil saturation of OML is 14.81%, with an oil-bearing volume of 0.2031%; the movable oil saturation of CLL is 9.93%, with an oil-containing volume (relative) of 0.1983%; the movable oil saturation of FQL is 7.65%, with an oil-containing volume (relative) of 0.2121%. Due to the oil-bearing properties and oil-bearing volume, TUL and FQL were determined to be the optimal laminae after a thorough evaluation.

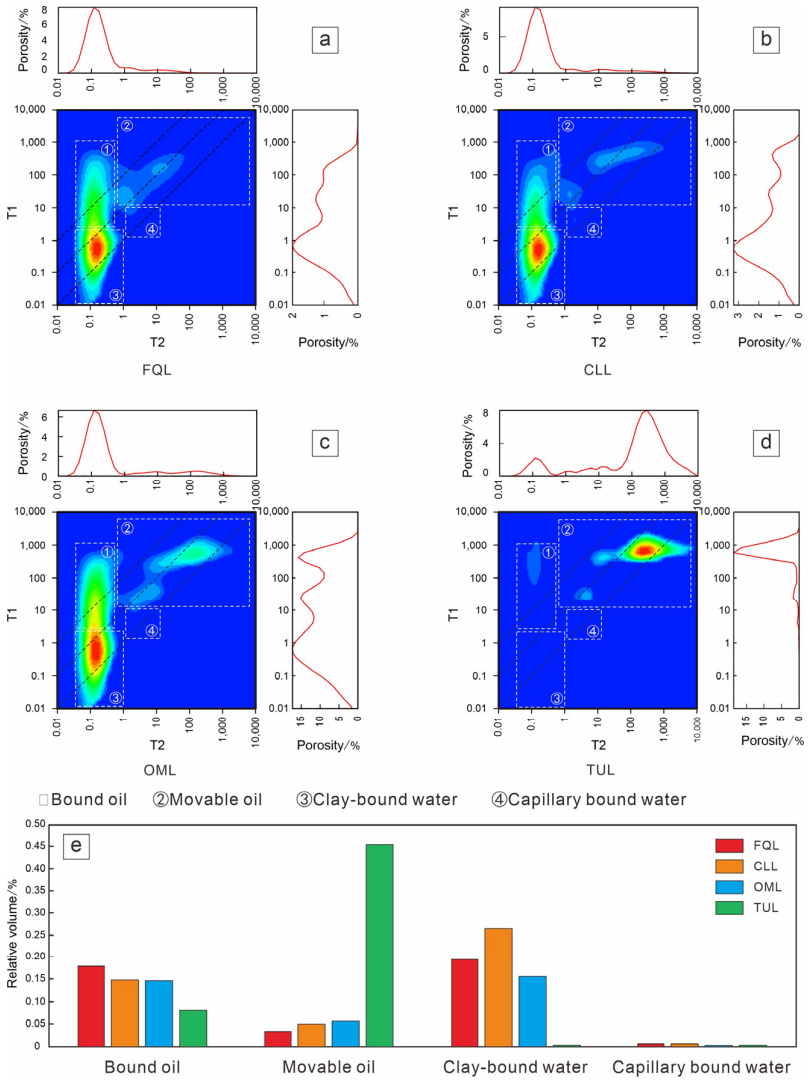


Figure 8. Laminae oil-bearing property of the Chang 7 Member in Ordos Basin. Oil content volume (relative) = (bound oil volume + movable oil volume)/pore volume × 100. (**a**) Oil-bearing property in Felsic laminae; (**b**) Oil-bearing property in Clay laminae; (**c**) Oil-bearing property in Organic matter laminae; (**d**) Oil-bearing property in Tuff laminae; (**e**) Oil content volume (relative volume) of different laminae.

5. Discussion

5.1. Being Rich in Organic Matter Guarantees a Sufficient Supply of Shale Oil

5.1.1. Reducibility and Suitable Continental Input

The paleoproductivity of the surface waters, the redox conditions, and the sedimentation rate are the key determinants of the organic matter enrichment in paleo-lacustrine sediments [20–23]. The examination of several elemental depositional environments reveals significant variances in the anomalously high organic matter-enriched intervals. The Chang 7_3 Member of the Well W336 has a high organic matter-enriched interval, according to the TOC data (Figure 9).

According to the climatic index C, the Chang 7_3 Member as a whole is going through warm, humid paleoclimatic conditions, which is also consistent with the overall positive tendency of anomalously high organic matter-enriched interval. Both the V/(V + Ni) and V/Cr ratios are low based on the redox conditions, suggesting a biased oxidizing environment. Sr/Ba indicated low values based on the salinity of the water, suggesting an overall biased desalination environment. Ti elemental signals from the continental inputs

displayed low values, demonstrating both the beneficial impact of suitable land source inputs on organic matter enrichment and the diluting effect of physical source inputs on organic matter. The P/Ti ratio is high, the organic matter-rich shale is associated with bioelement like iron, phosphorus, molybdenum, and uranium, and the abnormally high organic matter-rich portion displays a very high primary productivity level (Figure 10). Overall, the Chang 7_3 Member of the Ordos Basin experiences warm, humid weather with a freshwater-slightly-saline climate. The presence of reduction condition, suitable injection of continental debris sources, and high primary productivity levels provide the necessary foundational conditions for the anomalously high organic matter enrichment.

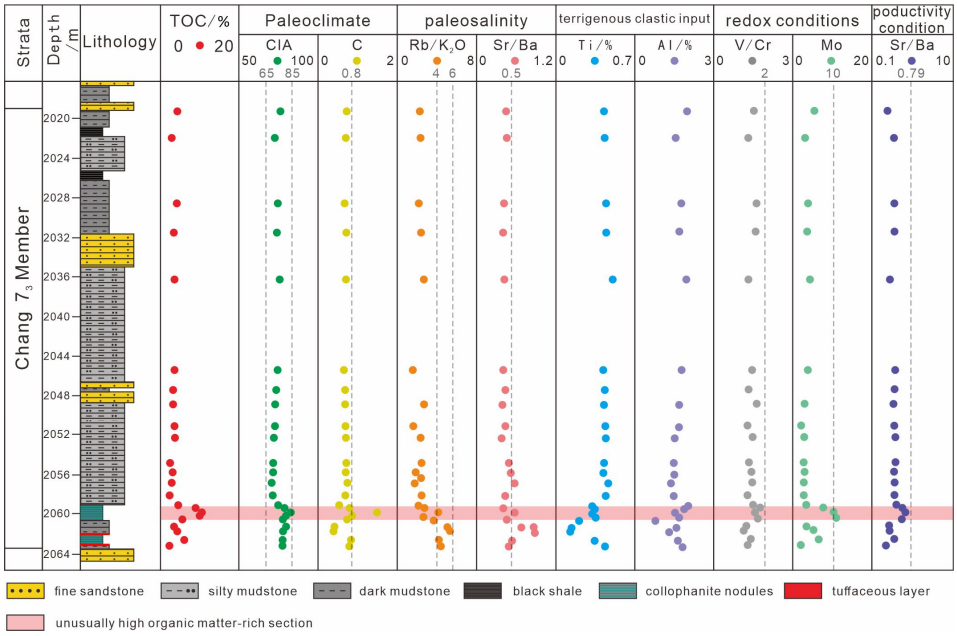


Figure 9. The comprehensive column map of element geochemical index of Chang 7_3 sub-member of Well Z40 in Ordos Basin (modified from [22]). CIA = [Al_2O_3/(Al_2O_3 + CaO* + Na_2O + K_2Ocorr)] × 100, K_2Ocorr = [m × Al_2O_3 + m × (CaO* + Na_2O)]/(1−m), CaO* is the residual calcium oxide content, m = K_2O/(Al_2O_3 + CaO* + Na_2O + K_2O), each component is expressed in moles, and the climate index C = ∑(Fe + Mn + Cr + Ni + V + Co)/∑(Ca + Mg + K+ Na + Sr + Ba).

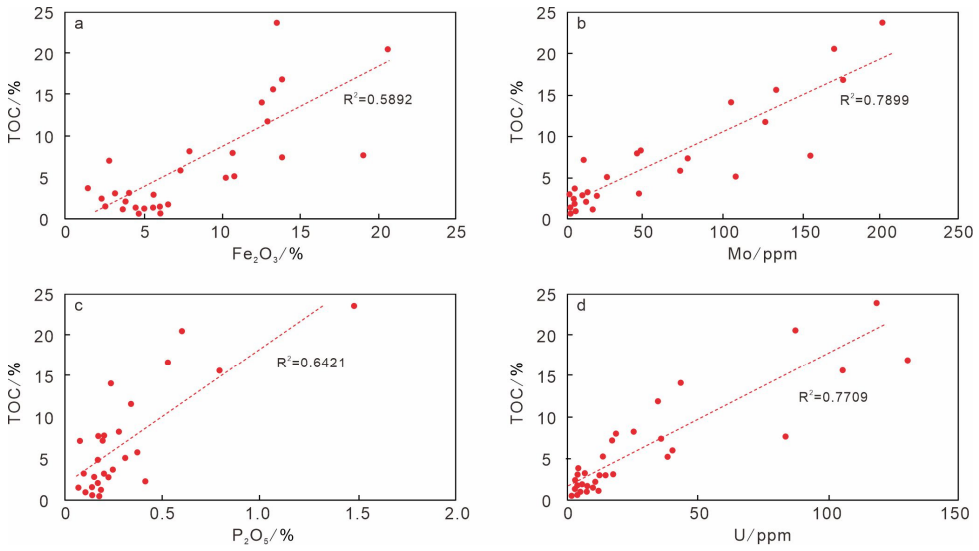


Figure 10. Nutrient element content versus TOC cross plate of the Chang 7 Member in Ordos Basin. (**a**) TOC and Fe_2O_3 intersection diagram; (**b**) TOC and Mo content intersection diagram; (**c**) TOC and P_2O_3 content intersection diagram. (**d**) TOC and U content intersection diagram.

5.1.2. Volcanic Event

Organisms can survive by obtaining nutrients from volcanic activity. The following is the control mechanism for the development of the organic matter-rich shale series in the Chang 7 Member, which has a direct connection to the occurrence of volcanic events during its depositional stage: (i) There are plenty of nutrients in the volcanic rocks, including calcium, iron, phosphorus, and nitrogen, which supply energy needed for organism survival [24–26]. (ii) The salinity and sulfur content of the water have a direct impact on the growth of algae, encouraging the growth of algae and the enrichment of nutrients. (iii) The enrichment of organic matter is favored by the modest volcanic activity. At the initiation of the eruption, as the amount of volcanic ash grows, so does the concentration of nutrients. Clearly, the Ba/Al and P/Ti ratios are high, and the amount of organic matter is elevated [26]. On the other hand, an environment that is hypoxic due to an excessive amount of volcanic ash deposition can result in widespread biological fatalities. As a result, dumping and diluting volcanic material took center stage, with Ba/Al, P/Ti, and organic matter content showing low values. In the later stages of volcanic activity, suitable ash content existed, presenting higher organic matter content.

5.1.3. Pyrite and Collophosphonite

A high content of feldspathic minerals indicates a strong continental input and pronounced dilution of organic matter enrichment (Figure 11a,b). The amount of feldspathic minerals shows the intensity of continental input. The samples with an abnormally high organic matter content in the Chang 7 Member have a low concentration of feldspathic minerals, and the majority of them have an abundance of collophosphonite minerals and strawberry pyrite (Figure 11c).

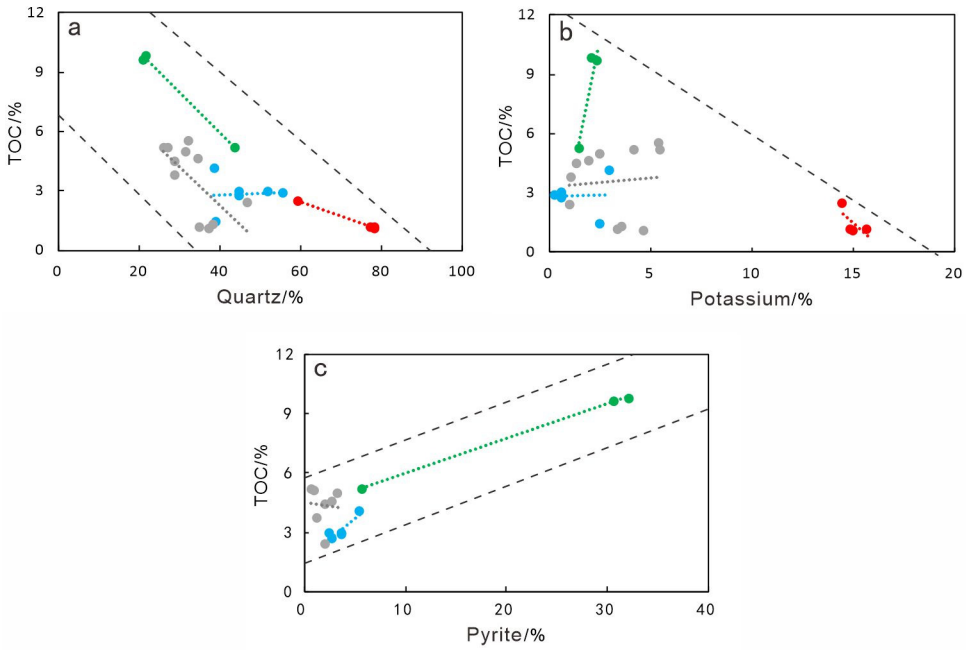


Figure 11. The characteristics of mineral composition of the Chang 7 Member in Ordos Basin. (**a**) TOC and quartz content intersection diagram; (**b**) TOC and potassium content intersection diagram; (**c**) TOC and pyrite content intersection diagram. The green, blue, red and grey lines are the data in felsic laminae, clay laminae, organic matter laminae and tuff laminae, respectively.

There is abundant spherical collophosphonite which is filled with phosphate minerals, organic matter, and minerals carrying chromium in the OML (Figure 12a–c). Richness of phosphorus nutrients can raise primary productivity and give organisms energy for

survival. Lower plankton with highly phosphorous shells or skeletons can directly generate collophosphonite by biological action. The production of OML with rich colophony in the Chang 7 Member is suggestive of the flourishing development of organisms throughout the formation period, as lower plankton generally forms very little collophosphonite by direct biological action.

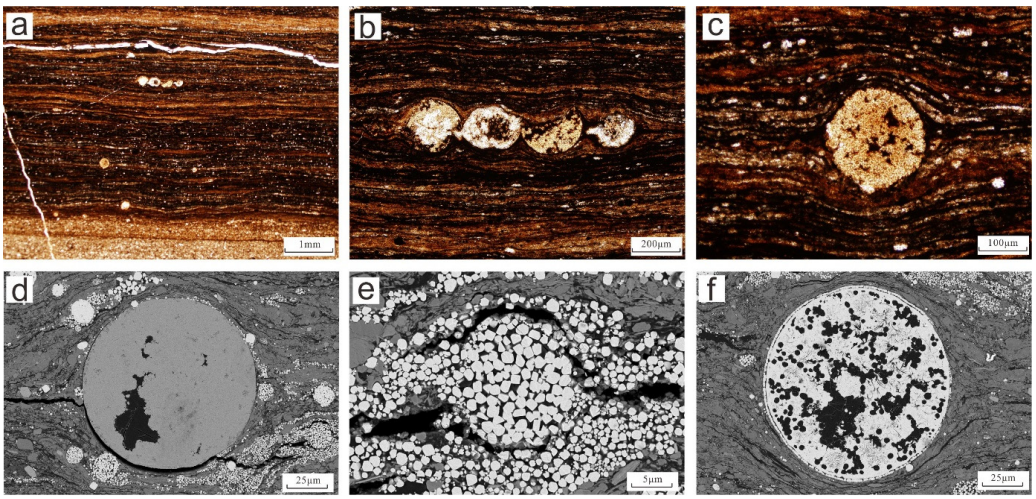


Figure 12. The characteristics of pyrite and cellophane in OML of the Chang 7 Member in Ordos Basin. (**a**) CLL–OML combination, polarizing microscope, Well W336, 2021.4 m; (**b**,**c**) cellophane, polarizing microscope, Well W336, 2021.4 m; (**d**) cellophane, SEM observation, Well W336, 2021.4 m; (**e**,**f**) pyrite, SEM observation, Well W336, 2021.4 m.

The relationship between pyrite and organic matter enrichment is illustrated in the following: (i) The large-scale formation of strawberry pyrite suggests a calm reducing condition that is ideal for the enrichment and preservation of organic materials. (ii) The significant amount of iron is needed to enrich pyrite, and the concentration of iron is directly correlated with the enrichment of organic matter [27,28]. (iii) Sulfate and reactive iron may play a key role in the formation of strawberry pyrite, suggesting that higher sulfur concentration encourages the growth of algae and the enrichment of organic matter.

The enrichment of organic matter is also influenced by the development of clay minerals (Figure 12d–f). Clay minerals are frequently found to have internally dispersed distributions and the development of organic matter populated with biogenic residues. They also have a large specific surface area, high charge, and ease of expansion between intervals [29,30]. In addition to organic matter adsorbed on the surface of clay minerals, clay minerals and organic matter can also be combined through physical and chemical adsorption to form organic clay complexes through the action of hydrogen bonding, ionic dipole force, electrostatic effect, and van der Waals force [31]. The cracking of clay minerals transformed to illite grows with increasing heat evolution, and organic matter gradually cracks to generate hydrocarbons. There is a negative association between the amount of illite and the content of organic carbon (Figure 12f).

5.2. The Production of Hydrocarbons Develops Pores and Contributes to Reservoir Quality

The dissolution pores in TUL and FQL, as well as the joint organic matter pores in CLL and OML, are the primary reservoir space in the Chang 7 Member. It was discovered that the hydrocarbon production of organic matter is favorable for pore formation to enhance reservoir space [32]. Moreover, the porosity may be increased by 4.9% by consuming 35% of shale with 7% TOC during the hydrocarbon generation evolution. It is particularly clear how organic matter hydrocarbon production contributes to porosity in the organic matter-rich shales of the Chang 7 Member in the Ordos Basin.

Using shale samples with a TOC of 5.8% from the Well FY2, Xiao et al. [33] performed diagenetic thermal simulation experiments and found that the primary factor influencing the evolution of shale pores is organic hydrocarbon generation, which also controls changes in pore volume and specific surface area. Not only does hydrocarbon discharge occur during the process of hydrocarbon generation, but the formation of organic matter pores and shrinkage fractures may also benefit the reservoir quality. Moreover, organic acids that support the formation of secondary dissolution pores can be produced by the pyrolysis of hydrocarbons, the decarboxylation reaction of kerogen, and the oxidation of oxidized minerals. The specific surface area and volume of mesopores and macropores exhibit an increasing trend under the influence of hydrocarbon generation when Ro is between 0.73% and 1.37%. At the same time, the high pressure generated by hydrocarbon generation can effectively prevent compaction from having a destructive effect.

Wu et al. conducted heating simulation experiments on shale with a buried depth of 2 452.6 m, a TOC of 2.23%, and a Ro of 0.67% in the Chang 7 Member in the Huachi area of the Ordos Basin. They found that the overall thermal evolution trend of irregular organic matter and massive organic matter was consistent [34]. Reservoir quality was significantly enhanced by the organic pores and micro-fractures that resulted from the pyrolysis and hydrocarbonization during the organic matter evolution process (Figure 13). The combination of organic hydrocarbon pores and inorganic mineral pores provides a significant amount of storage space for shale oil. The production of organic hydrocarbons in the shale series in the Chang 7 Member of the Ordos Basin significantly improves the physical features of the reservoir.

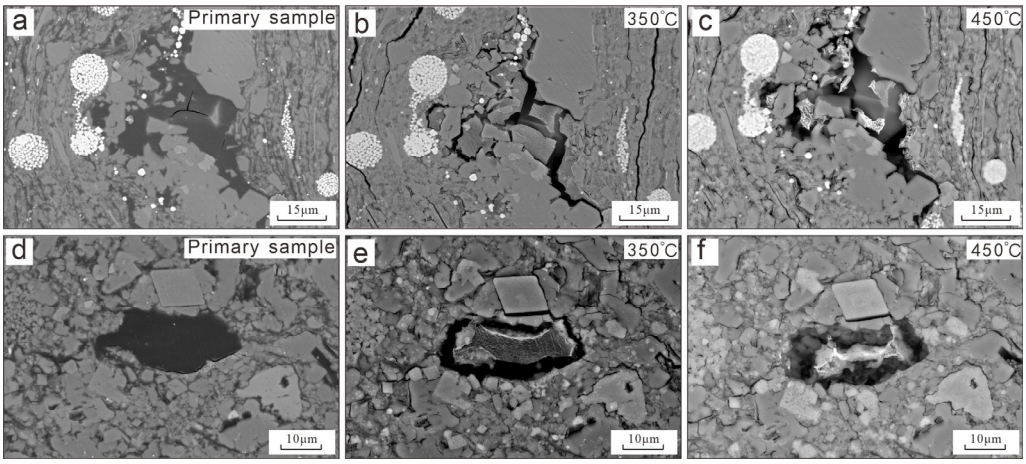


Figure 13. Hydrocarbon generation evolution of organic matter of the Chang 7 Member in Ordos Basin (modified from [34]).

5.3. The "Clay Generation-Siliceous Reservoir" Shale Oil Enrichment Model

Based on the laminae combinations, this study analyzed the crude oil micromigration paths and occurrence characteristics under the control of the shale laminae in the Chang 7 Member of the Yanchang Formation in the Ordos Basin by using laser confocal microscopy and nitrogen adsorption and pyrolysis data pre- and post-oil washing.

In the FQL–CLL combination, the TOC value of the CLL (TOC = 3.95%, $S_1 + S_2$ = 13.86 mg/g) is higher than that of the FQL (TOC = 2.11%, $S_1 + S_2$ = 16.98 mg/g), and the light hydrocarbon components (24.49%) and heavy hydrocarbon components (28.47%) are obviously concentrated in the FQL (Figure 14). Combined with the measurement of pore plane porosity of CLL, FQL being 0.206% and 0.514%, respectively, indicates the micromigration of hydrocarbons from the CLL to the FQL after hydrocarbon generation in the CLL. For the TUL–OML combination, the TOC value of the OML (TOC = 9.63%)

is higher than that of the TUL (TOC = 1.22%), and the light hydrocarbon components (32.18%) and heavy hydrocarbon components (34.04%) are obviously concentrated in the TUL. This indicates the micromigration of hydrocarbons from the OML to the TUL after hydrocarbon generation in the OML. For the FQL–OML combination, the heavy hydrocarbon components are concentrated in the FQL. This indicates the micromigration of hydrocarbons from the OML to the FQL after hydrocarbon generation. In addition, the crude oil signal in the OML shows that the OML is pressurized by hydrocarbon generation and produces overfracturing fractures in the OML, which provides a reservoir space for crude oil enrichment.

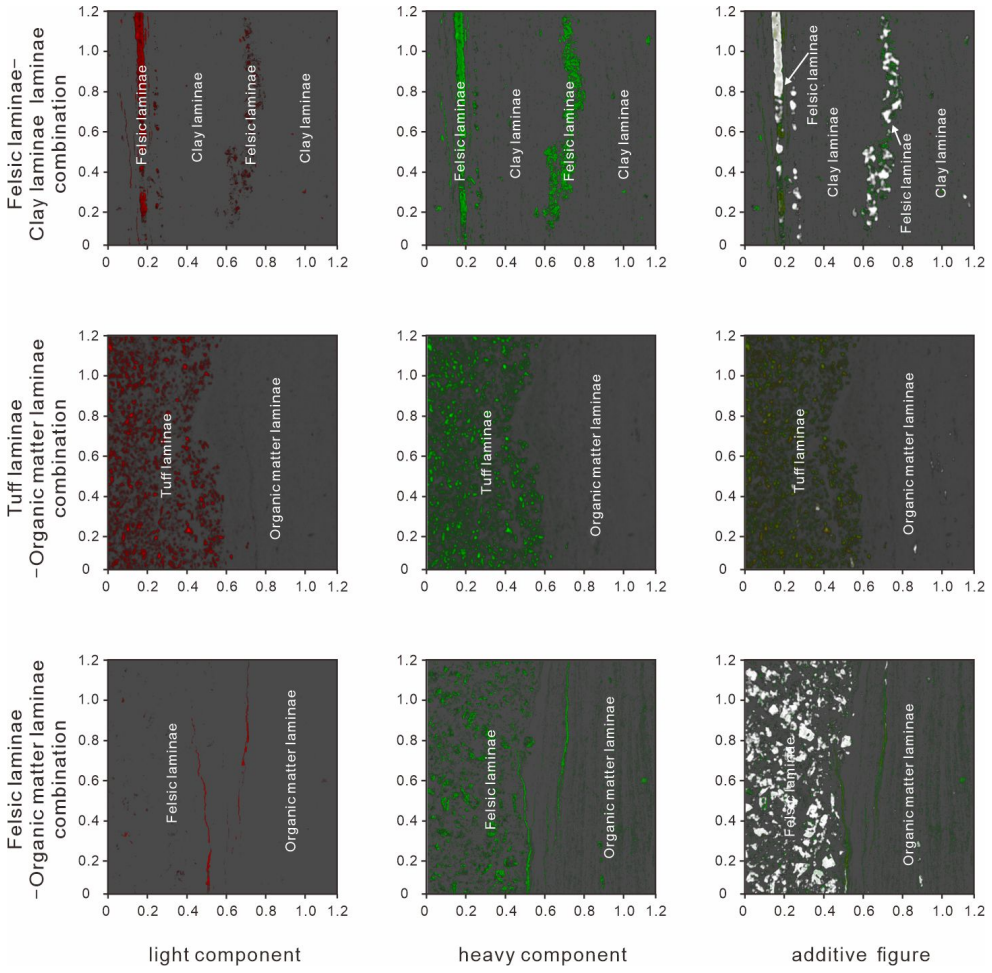


Figure 14. Laminae oil-bearing property of the Chang 7 Member in Ordos Basin.

Based on pre- and post-oil washing data, the pore volume increased most after oil washing in the TUL (Figure 15). And the pore volume increase in the pore size range of different laminae that greater than 10 nm accounted for 83%~92% of the total pore volume increase, indicating the lower limit of the pore volume of shale oil in the Chang 7 Member of the freshwater lacustrine condition is about 10 nm.

Macroscopic and mesopore pore sizes dominated FQL. The pore volume of pores that have a pore diameter smaller than 32 nm decreased significantly after hexane oil washing; the pore volume of pores larger than 32 nm did not change significantly, and the pore volume decreased again after dichloromethane oil washing (Figure 16). The analysis revealed that following hexane oil washing, the light polar oil that had filled the pores was washed out. As a result, the pore diameter of mesopores smaller than 32 nm increased, with some of them increasing to 32 and 128 nm, while the pore diameter of pores larger than 32 nm also increased following oil washing, with some increasing to exceeding 128 nm.

Following dichloromethane oil washing, the heavy polar oil that had filled the pores was washed out. The pores throughout the entire pore diameter range exhibited a tendency to enlarge, and the pores larger than 128 nm significantly increased. This resulted in a decrease in the pore volume. One of the main causes of the two extractive desorption processes of decreased pore volume in FQL is the conversion of mesopores to macropores following oil washing.

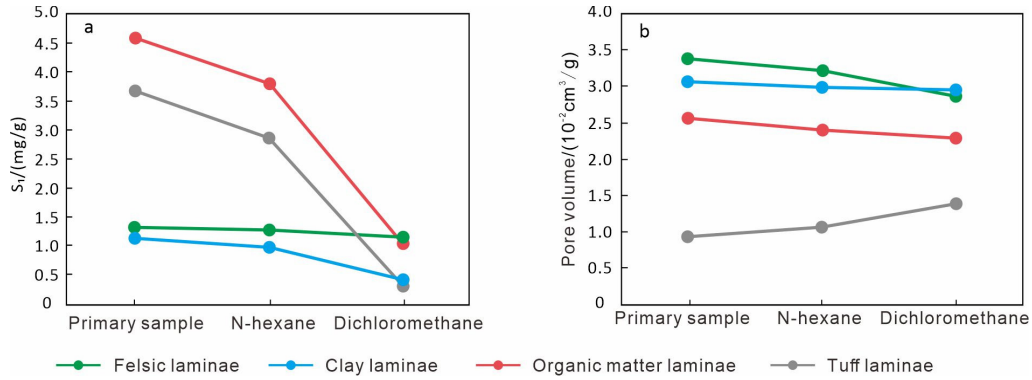


Figure 15. Laminae geochemical characteristics and pore volume before and after oil washing of the Chang 7 member in Ordos Basin. (**a**) S_1 before and after oil washing of the Chang 7 member in Ordos Basin; (**b**) Pore volume before and after oil washing of the Chang 7 member in Ordos Basin.

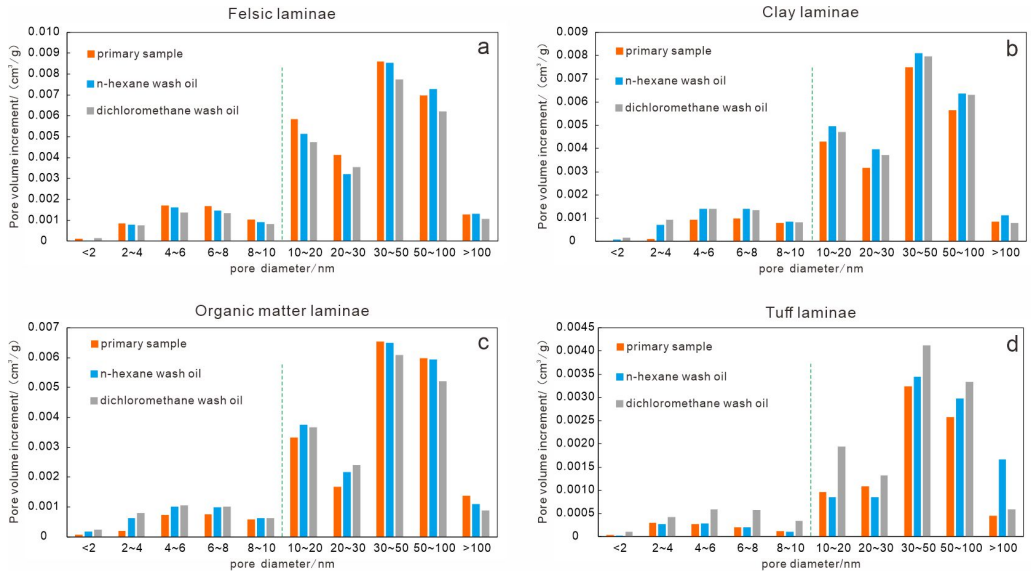


Figure 16. Laminae pore volume before and after oil washing of the Chang 7 Member in Ordos Basin. (**a**) Laminae pore volume before and after oil washing in Felsic laminae; (**b**) Laminae pore volume before and after oil washing in Clay laminae; (**c**) Laminae pore volume before and after oil washing in Organic matter laminae; (**d**) Laminae pore volume before and after oil washing in Tuff laminae.

Mesopores predominated in CLL, with macropores serving as a supplement. However, the pore diameters were smaller than those of FQL. Following oil washing, there was no discernible change in the pore volume in the range of 30~50 nm (Figure 16), and the overall trend of pore volume decrease was less than that of FQL. The pore volumes in the CLL with pore diameter ranges smaller than 30 nm and larger than 50 nm had a tendency to increase. Because S1 value in CLL was lower than that of FQL, it can be concluded that CLL had less hydrocarbon content overall.

Following oil washing in OML, the desorption pore volume shrank, and following oil washing in n-hexane, the pore volume in the range of less than 28 nm greatly increased (Figure 16), primarily as a result of the weak polar oil discharging from the pores with tiny

pore diameter. After two oil washes, the pore volume in the pore size range larger than 40 nm showed a decreasing trend. The main cause was that the pore diameter was continuously expanding larger than 128 nm, and this portion of the pore was originally endowed with weakly polar and strongly polar oils, which were discharged after two oil washes.

The highest oil content was found in TUL; 95% of the pores had pore diameter larger than 100 nm, and after the oil was washed out, the volume of detached pores altered the most and grew with time (Figure 16). After washing the oil with dichloromethane, the average pore diameter and the pore volume of detached pores increased in TUL, while the pores less than 20 nm showed a decreasing pore volume, but the pores larger than 50 nm show the opposite.

After washing out light polar oil, the pore diameter of TUL was found to be larger overall. After washing out heavy polar oil, the pore diameter increased but remained within the range of less than 20 nm overall. In some cases, the pore diameter of less than 20 nm increased to greater than 20 nm. On the one hand, the washing out of light and heavy polar oils increased the pore volume of the pores with pore diameter larger than 50 nm. On the other hand, the hydrocarbon washing out caused the pore diameter of the pores that were initially smaller than 50 nm to increase.

According to the FIB-SEM data (Figure 17), inorganic pores predominate in the FQL, whereas organic pores predominate in the OML. The fraction of inorganic mineral pores and organic pores in the CLL are 58% and 42%, respectively. The TUL has a significant number of inorganic mineral dissolution pores, as seen by SEM observation. In the Chang 7 Member of the Ordos Basin, there is a significant development of inorganic pores together with reliable organic hydrocarbon production. The pores created as a result of the organic hydrocarbon generation process significantly enhance the physical characteristics of the reservoir. The combination of organic pores and inorganic pores provides a large amount of occurrence space for shale oil.

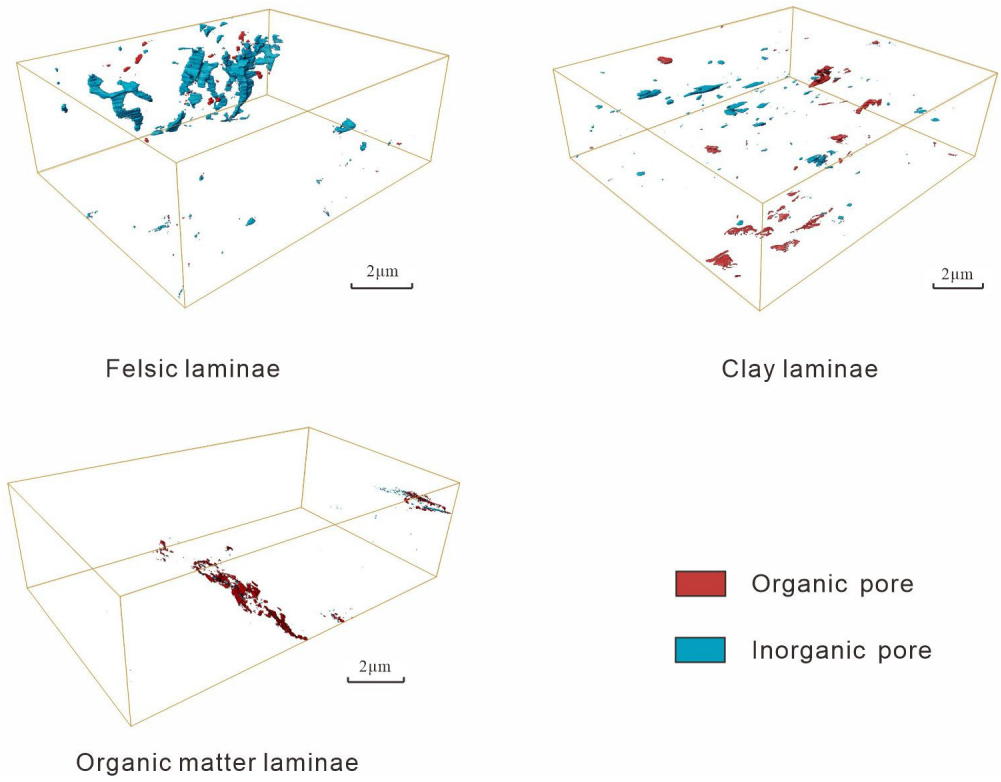


Figure 17. Three-dimensional pore model of laminae in the Chang 7 Member, Ordos Basin.

Generally, the main source laminae in the Chang 7 Member of the Ordos Basin of the freshwater lacustrine condition are the OML and CLL, while the main reservoir laminae are the FQL and TUL. Some of the hydrocarbons produced by hydrocarbon generation are stored in the pore space inside the laminae, while the majority migrate to the inorganic pores of the adjacent FQL and TUL. In the FQL–OML and FQL–CLL combinations, hydrocarbons are dominated by micromigration within the lamina combination. Organic acids are produced during the burial and evolution of the organic matter hydrocarbon generated leading to the formation of feldspar dissolution pores (Figure 18). The FQL has a high concentration of clay and felsic minerals. During the compaction process, the felsic particles provide support and some intergranular pores occur. In addition, clay minerals undergo transformation and dehydration, and a significant number of clay mineral intragranular pores develop. The hydrocarbons produced by the OML/CLL micromigrate to the FQL as burial depth and temperature increase. These hydrocarbons are primarily stored in the intragranular pores of clay mineral particles in both the free and adsorption states, and they primarily exist in the adsorption state in the feldspar dissolution pores. The organic matter enters the stage of thermal evolution and hydrocarbon generation as burial depth and temperature rise. The produced crude oil is then transported to the TUL, where the majority of it dissolves into free-state dissolution pores and some of it is stored in the intragranular pores of pyrite particles and clay mineral in both the free-state and adsorption states. It confirms that OML and CLL afford abundant shale oil, the combination of organic pores and inorganic pores in FQL and TUL serve as reservoir space, and the "clay generation-siliceous reservoir" shale oil enrichment model applies in freshwater lacustrine basins.

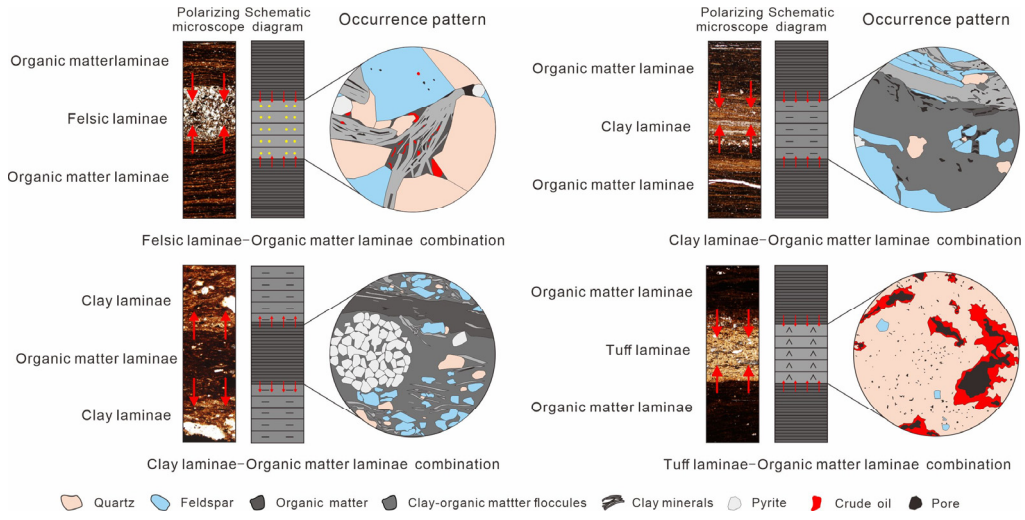


Figure 18. Shale oil micromigration model in the Chang 7 Member, Ordos Basin.

A high-quality shale oil enrichment has occurred in the Chang 7 Member of the Ordos Basin, under the total management of hydrocarbon generation, storage, and late preservation conditions. High organic matter content in the hydrocarbon source rock, substantial sulfate reduction, high paleo-productivity, and strong hydrocarbon potential are all present in the Chang 7 Member. Both inorganic and organic pores develop, with the degree of thermal evolution influencing the formation of organic pores. These pores have high porosity and are filled with hydrocarbons for an extended period of time. There is little destruction of the reservoir space because the uplift period is late and the uplift amplitude is moderate. A guarantee for effective shale oil enrichment and reservoir formation is provided by the effective matching of hydrocarbon production, storage, and preservation conditions.

6. Conclusions

There are four types of laminae in the Chang 7 Member, Yanchang Formation, Ordos Basin, which are feldspar-quartz laminae (FQL), clay laminae (CLL), organic matter laminae (OML), and tuff laminae (TUL), respectively. The shale laminae exhibit significant differences and form four distinct types of laminae combinations: the FQL–CLL combination, the FQL–OML combination, the CLL–OML combination, and the TUL–OML combination.

The reservoir space of the Chang 7 Member is dominated by dissolution pores, intragranular pores, organic pores, and microfractures, and the porosity shows TUL > FQL > CLL > OML. The porosity is mainly contributed by mesoporous and macroporous porosity, and mesopores have obvious advantages in the number of pores. The pore diameter of TUL is primarily composed of micrometer-sized secondary pores that are generated during the diagenesis process, while mesopore and macropore development is dominant in FQL.

The main source laminae in the Chang 7 Member of the Ordos Basin are the OML and CLL, while the main reservoir laminae are the FQL and TUL. Some of the hydrocarbons produced by hydrocarbon generation are stored in the pore space inside the laminae, while the majority migrate to the inorganic pores of the adjacent FQL and TUL. It confirms that OML and CLL afford abundant shale oil, the combination of organic pores and inorganic pores in FQL and TUL serve as reservoir space, and the "clay generation-siliceous reservoir" shale oil enrichment model applies in the Chang 7 Member of Ordos Basin.

Author Contributions: M.L.: conceptualization, writing—review & editing, methodology, formal analysis, writing—original draft. W.L.: formal analysis, writing—review & editing, project administration. M.G.: data curation, writing—review & editing, formal analysis. S.W.: resources, writing—review & editing, formal analysis, funding acquisition. P.W.: software, writing—review & editing, formal analysis. Y.W.: investigation, writing—review & editing, formal analysis. Q.C.: supervision, writing—review & editing, formal analysis. Z.X.: visualization, writing—review & editing, supervision. Y.H.: methodology, writing—original draft, supervision. All authors have read and agreed to the published version of the manuscript.

Funding: This research received no external funding.

Data Availability Statement: The original contributions presented in this study are included in the article. Further inquiries can be directed to the corresponding author.

Conflicts of Interest: Authors Mengying Li, Wenzheng Li, Mingfeng Gu, Pengwan Wang, Yuce Wang, Quanbin Cao, Zhehang Xu and Yi Hao were employed by the PetroChina Hangzhou Institute of Petroleum Geology. Authors Songtao Wu are employed by the China National Petroleum Corporation (CNPC). The remaining authors declare that the research was conducted in the absence of any commercial or financial relationships that could be construed as a potential conflict of interest.

References

1. Liu, B.; Shi, J.X.; Fu, X.F.; Lyu, Y.; Sun, X.; Gong, L.; Bai, Y. Petrological characteristics and shale oil enrichment of lacustrine fine-grained sedimentary system: A case study of organic-rich shale in first member of Cretaceous Qingshankou Formation in Gulong Sag, Songliao Basin, NE China. *Pet. Explor. Dev.* **2018**, *45*, 828–838. [CrossRef]
2. Zhao, X.Z.; Zhou, L.H.; Pu, X.G.; Jin, F.; Shi, Z.; Xiao, D.; Han, W.; Jiang, W.; Zhang, W.; Wang, H. Favorable formation conditions and enrichment characteristies of lacustrine facies shale oil inl faulted lake basin:a case study of Member 2 of Kongdian Formation in Cangdong sag, Bohai Bay Basin. *Acta Pet. Sin.* **2019**, *40*, 1013–1029.
3. Xi, K.L.; Li, K.; Cao, Y.C.; Lin, M.; Niu, X.; Zhu, R.; Wei, X.; You, Y.; Liang, X.; Feng, S. Laminae combination and shale oil enrichment patterns of Chang 73 sub-member organic-rich shales in the Triassic Yanchang Formation, Ordos Basin, NW China. *Pet. Explor. Dev.* **2020**, *47*, 1244–1255. [CrossRef]
4. Li, T.T.; Zhu, R.K.; Bai, B.; Chongxiao, W.; Tiefeng, L. Characteristics and Research Significance of Fine Lacustrine Sedimentary Rock Laminations of Xiagou Formation in Qingxi Depression of Jiuquan Basin. *China Pet. Explor.* **2015**, *20*, 38–47.
5. Li, C.; Cao, Y.C.; Jiang, Z.X.; Wu, J.; Guoqi, S.; Wang, Y. Shale oil potential of lacustrine black shale in the Eocene Dongying depression: Implications for geochemistry and reservoir characteristics. *AAPG Bull.* **2017**, *101*, 1835–1858. [CrossRef]

6. Liu, B.; Bai, L.H.; Chi, Y.A.; Jia, R.; Fu, X.; Yang, L. Geochemical characterization and quantitative evaluation of shale oil reservoir by two-dimensional nuclear magnetic resonance and quantitative grain fluorescence on extract: A case study from the Qingshankou Formation in Southern Songliao Basin, northeast China. *Mar. Pet. Geol.* **2019**, *109*, 561–573. [CrossRef]
7. Hu, S.Y.; Zhao, W.Z.; Hou, L.H.; Yang, Z.; Zhu, R.; Wu, S.; Bai, B.; Jin, X. Development potential and technical strategy of continental shale oil in China. *Pet. Explor. Dev.* **2020**, *47*, 819–828. [CrossRef]
8. Fu, S.T.; Jin, Z.J.; Fu, J.H.; Li, S.; Yang, W. Transformation of understanding from tight oil to shale oil in the Mem-l ber 7 of Yanchang Formation in Ordos Basin and its significance of exploration and development. *Acta Pet. Sin.* **2021**, *42*, 561–569.
9. Kuang, L.C.; Hou, L.H.; Yang, Z.; Wu, S. Key parameters and methods of lacustrine shale oil reservoir characterization. *Acta Pet. Sin.* **2021**, *42*, 1–14.
10. Li, M.Y.; Zhu, R.K.; Hu, S.Y. Geological characteristics and resource potential of overseas terrestrial shale oil. *Lithol. Reserv.* **2022**, *34*, 163–174.
11. Sonnenberg, S.A.; Pramudito, A. Petroleum geology of the giant Elm Coulee field, Williston Basin. *AAPG Bull.* **2009**, *93*, 1127–1153. [CrossRef]
12. Du, J.H.; Hu, S.Y.; Pang, Z.L.; Lin, S.; Hou, L.; Zhu, R. The types, potentials and prospects of continental shale oil in China. *China Pet. Explor.* **2019**, *24*, 560–568.
13. Krumbein, W.C. The dispersion of fine-grained sediments for mechanical analysis. *J. Sediment. Res.* **1933**, *3*, 121–135. [CrossRef]
14. Tucker, M.E. *Sedimentary Petrology: An Introduction to the Origin of Sedimentary Rocks*; Blackwell Scientific Publication: Hoboken, NJ, USA, 2001; p. 260.
15. Macquaker, J.H.S.; Adams, A.E. Maximizing Information from Fine-Grained Sedimentary Rocks: An Inclusive Nomenclature for Mudstones. *J. Sediment. Res.* **2003**, *73*, 735–744. [CrossRef]
16. Schieber, J.; Southard, J.; Thaisen, K. Accretion of Mudstone Beds from Migrating Floccule Ripples. *Science* **2007**, *318*, 1760–1763. [CrossRef]
17. Aplin, A.C.; Macquaker, J.H.S. Mudstone diversity: Origin and implications for source, seal, and reservoir properties in petroleum systems. *AAPG Bull.* **2011**, *95*, 2031–2059. [CrossRef]
18. Liu, G.H.; Huang, Z.L.; Jiang, Z.X.; Chen, J.; Chen, C.; Gao, X. The characteristic and reservoir significance of lamina in shale from Yanchang Formation of Ordos Basin. *Nat. Gas Geosci.* **2015**, *26*, 408–417.
19. Milliken, K. A Compositional Classification for Grain Assemblages in Fine-Grained Sediments and Sedimentary Rocks-Reply. *J. Sediment. Res.* **2016**, *84*, 1185–1199. [CrossRef]
20. Caplan, M.L.; Bustin, M.R. Devonian—Carboniferous Hangenberg mass extinction event widespread organic-rich mudrock and anoxia: Causes and consenuences. *Palaeogeogr. Palaeoclimatol. Palaeoecol.* **1999**, *148*, 187–207. [CrossRef]
21. Mort, H.; Jacquat, O.; Adattte, T.; Steinmann, P.; Föllmi, K.; Matera, V.; Berner, Z.; Stüben, D. The Cenomanian/Turonian anoxic event at the Bonarelli Level in Italy and Spain: Enhanced productivity and/or better preservation. *Cretac. Res.* **2007**, *28*, 597–612. [CrossRef]
22. Liu, H.L.; Zou, C.N.; Qiu, Z.; Pan, S.; Zhang, W.; Jing, Z.; Hao, J.; Yin, S.; Wu, S.; Li, S.; et al. Sedimentary enrichment factors of extraordinarily high organic matter in the sub-member 3 of Member 7 of Yanchang Formation, Ordos Basin. *Acta Pet. Sin.* **2022**, *43*, 1520–1541.
23. Liu, Q.Y.; Li, P.; Jiang, L.; Jin, Z.; Liang, X.; Zhu, D.; Pang, Q.; Zhang, R.; Liu, J. Distinctive volcanic ash–rich lacustrine shale deposition related to chemical weathering intensity during the Late Triassic: Evidence from lithium contents and isotopes. *Sci. Adv.* **2024**, *10*, eadi6594. [CrossRef]
24. Demaison, G.J.; Moore, G.T. Anoxic Environments and Oil Source Beds Genesis. *AAPG Bull.* **1980**, *2*, 1179–1209. [CrossRef]
25. Duggen, S.; Croot, P.; Schacht, U.; Hoffmann, L. Subduction zone volcanic ash can fertilize the surface ocean and stimulate pHytoplankton growth: Evidence from biogeochemical experiments and satellite data. *Geophys. Res. Lett.* **2007**, *34*, 95–119. [CrossRef]
26. Liu, Q.Y.; Li, P.; Jin, Z.J.; Sun, Y.; Hu, G.; Zhu, D.; Huang, Z.; Liang, X.; Zhang, R.; Liu, J. Organic-rich formation and hydrocarbon enrichment of lacustrine shale strata: A case study of Chang 7 Member. *Earth Sci.* **2022**, *65*, 118–138. [CrossRef]
27. Berner, R.A.; Leeuw, J.W.D.; Spiro, B.; Murchison, D.G.; Eglinton, G. SulpHate reduction, organic matter decomposition and pyrite formation (and discussion). *Philos. Trans. R. Soc. Lond.* **1985**, *315*, 25–38.
28. Liu, J.Y.; Li, S.X.; Li, Z.; Liu, Q.; Guo, W.; Zhou, X.; Ma, X. Characteristics and geological significance of pyrite in Chang 73 sub-member in the Ordos Basin. *Nat. Gas Geosci.* **2021**, *32*, 1830–1838.
29. Miao, J.Y.; Zhu, Z.Q.; Liu, W.R.; Lu, H.Y. Occurrence of Organic Matter and Its Effect on Sealing Ability of Argillaceous Rock. *Acta Sedimentol. Sin.* **1999**, *17*, 478–481.
30. Zhang, L.Y.; Kong, X.X.; Zhang, C.R.; Wen, Z.; Xingyou, X.; Zheng, L. High-quality oil-prone source rocks in Jiyang Depression. *Geochimica* **2003**, *32*, 35–42.
31. George, C. Formation and Properties of Clay-Polymer Complexes 2nd edition. *Clay Miner.* **2014**, *9*, 123–124.

32. Jarvie, D.M.; Hill, R.; Ruble, T.E.; Pollastro, R.M. Unconventional shale-gas systems: The Mississippian Barnett Shale of north-central Texas as one model for thermogenic shale-gas assessment. *AAPG Bull.* **2007**, *91*, 475–499. [CrossRef]
33. Xiao, L.; Li, Z.; Yang, Y.D.; Tang, L.; Wan, C.; Liang, Z.; Yu, H.; Hou, Y.; Wang, L. Pore evolution model and influencing factors of continental shale in Yanchang Formation, Ordos Basin. *Sci. Technol. Eng.* **2020**, *20*, 8122–8132.
34. Wu, S.T.; Zhu, R.K.; Cui, J.G.; Cui, J.; Bai, B.; Zhang, X.; Jin, X.; Zhu, D.; You, J.; Li, X. Characteristics of lacustrine shale porosity evolution, Triassic Chang 7 Member, Ordos Basin, NW China. *Pet. Explor. Dev.* **2015**, *42*, 167–176. [CrossRef]

Disclaimer/Publisher's Note: The statements, opinions and data contained in all publications are solely those of the individual author(s) and contributor(s) and not of MDPI and/or the editor(s). MDPI and/or the editor(s) disclaim responsibility for any injury to people or property resulting from any ideas, methods, instructions or products referred to in the content.